A major purpose of the Technical Information Center is to provide the broadest dissemination possible of information contained in DOE's Research and Development Reports to business, industry, the academic community, and federal, state and local governments.

Although a small portion of this report is not reproducible, it is being made available to expedite the availability of information on the research discussed herein.

LA-UR -86-943 CONF-8604147--3 Received by OSTI

APR 07 1986

LA-UR--86-943

DE86 008740

TITLE EXPERIMENTAL MEASUREMENT OF ABLATION EFFECTS IN PLASMA ARMATURE RAILGUNS

AUTHOR(S) Jerald V. Parker, P-7
William M. Parsons, CIR-9

SUBMITTED TO 3rd Symposium of Electromagnetic Launch Technology
April (20-24), 1986, Austin, TX.

DISCLAIMER

Los Alamos Los Alamos National Laboratory
Los Alamos, New Mexico 87545

MASTER

FORM NO 836 R4

DISTRIBUTION OF THIS DOCUMENT IS UNLIMITED

EXPERIMENTAL MEASUREMENT OF ABLATION EFFECTS IN PLASMA ARMATURE RAILGUNS

Jerald V. Parker and W. Mark Parsons

Abstract - Experimental evidence supporting the importance of ablation in plasma armature railguns is presented. Experiments conducted using the HYVAX and MIDI-2 railguns are described. Several indirect effects of ablation are identified from the experimental results. An improved ablation model of plasma armature dynamics is proposed which incorporates the restrike process.

INTRODUCTION

Since the first demonstration of a plasma armature railgun in 1977 [1] there has been little progress made in achieving the ultrahigh velocities which many investigators have sought. It is now generally recognized that the performance of a plasma armature railgun is strongly degraded by wall ablation effects at velocities greater than 5-10 km/s. Experimental measurements on the HYVAX railgun at Los Alamos in 1984 [2] and subsequent analysis [3] have shown that most of the observed performance loss can be accounted for by four physical mechanisms which are direct or indirect consequences of wall ablation.

These processes are:

1) Viscous drag
2) Arc restrike
3) Kinetic drag ($\dot{m}v$ effect)
4) Armature mass increase

The relative importance of these processes is approximately in the order listed, although arc restrike may dominate in some experiments.

In reference [2,3] the validity of the ablation model is supported by comparing the measured projectile position versus time to computer simulation made using the LARGE code including ablation. Recently, this comparison has been extended to include a broad range of railgun experiments [4]. Close agreement between theory and experiment, without any adjustable parameters in the ablation model, is a persuasive but indirect argument favoring the ablation model. The major shortcoming of the ablation model is its failure to treat the arc restrike process. In this paper more direct evidence supporting the importance of ablation processes is described and the relationship between ablation and restrike is developed.

The first section deals with measurements made on the HYVAX railgun. In particular, detailed measurements of the rail current waveform are presented and analyzed to provide data on plasma armature current distribution.

The second section presents recent results from experiments on the MIDI-2 railgun using the "free arc" technique to investigate ablation at high velocity (up to 11 km/s). At high velocity only insulator ablation is observed and the maximum arc velocity scales approximately as the inverse square root of the average molecular weight of the insulator material. Finally, the restrike arc and its connection with ablation is examined in detail. The important processes leading to restrike are identified and an improved ablation model is proposed.

Manuscript received

Work supported by U.S. Department of Energy and the U.S. Army, Ballistic Missile Defense Advanced Technology Center

The authors are with Los Alamos National Laboratory, Los Alamos, NM 87545

HYVAX EXPERIMENTS

HYVAX-I railgun

The HYVAX railgun was designed to be a five stage, distributed device for hypervelocity technology development. Mechanically it was to consist of nine 1.22 m sections and seven 0.3 m sections which contained feedthroughs for current input. These sections could be assembled in any order to obtain the optimum current profile in the railgun. The full HYVAX railgun was never assembled.

HYVAX-I is the phase I configuration of HYVAX, a single stage railgun with three power input modules at the breech end and two 1.22 m modules comprising the barrel. The usable acceleration length is 2.4 m.

The HYVAX rail configuration is shown in Fig. 1. The bore diameter at assembly is nominally 10.8 mm and the inductance gradient is L' = 0.30 μH/m. A reaming fixture is utilized to finish the bore to an accurate diameter. Reamers are available in increments of 1.3 mm up to 12.7 mm. Experiments discussed below have been conducted for various diameters from 10.1 to 11.4 mm. The main insulator material which supports the rails and sidewalls is a unidirectional fiberglass epoxy composite. Various sidewall inserts have been evaluated experimentally. In addition to the fiberglass-epoxy material these include G-10, Lexan, and Mycalex. The external shell of the barrel is a 12.7 cm i.d. steel tube which provides mechanical support for the internal structure and provides a reliable vacuum-tight container.

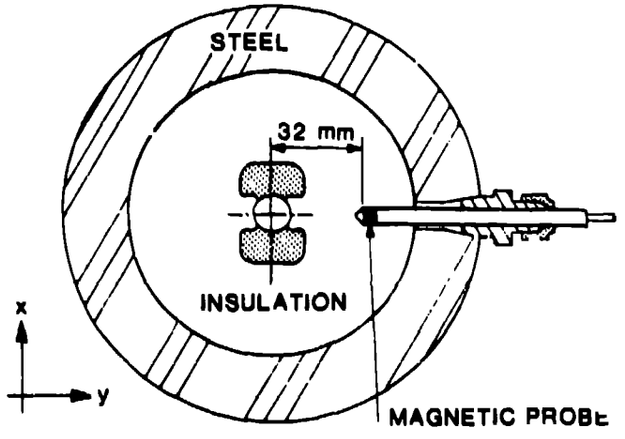

Fig. 1 Cross section of the HYVAX railgun

Injector An injector is used for all HYVAX tests. The injector barrel is a 3.2 mm i.d. steel tube 38 cm long. The bore is reamed concentric with the railgun bore. Three different breech assemblies are used with this barrel depending upon the driving medium. The driving media available are:

1) Plasma - A polyethylene plasma generated by a 15 kJ electrical discharge.
2) Chemical - Double-based pistol powder (typically 43.5 grains) with electrical ignition.
3) Helium - A 1000 PSI helium reservoir with electrically activated burst diaphragm.

Timing For most experiments the electrical discharge was triggered by a preset time delay generator. This was generally satisfactory because all three injectors had very reproducible acceleration characteristics. Attempts to use a laser triggering system were unsuccessful because the signal was not reliable. Laser attenuation waveforms were recorded and used to measure injection velocity. For some of the later tests a pair of fast pressure switches was used to sense projectile position and to provide a reliable trigger signal.

Fusing For most experiments the fuse consisted of 10-12 turns of 0.2 mm diameter steel wire wound in a circumferencial groove at the rear edge of the projectile. This form of fuse provided much more reliable contact than the conventional metal foil bonded to the back surface of the projectile. A few experiments were performed with a static fuse consisting of a 0.05 mm thick copper foil recessed into the wall of the railgun.

Electrical System Three capacitor bank modules provide electrical power to the breech of HYVAX-I. Each module has a capacitance of 1.3 mF and a maximum operating voltage of 20 kV. Two of the three modules have an 11 μH inductor to limit their peak current to 175 kA. The third module has a 45 μH inductor and a maximum current of 80 kA. A typical current waveform for these three modules is shown by the curve marked "input current" in Fig. 2. The low current module is triggered at 200 μs to provide an approximately flat-top current waveform.

Diagnostics The diagnostics listed in Table I were routinely used on each HYVAX test. Great care was taken to isolate the measuring apparatus from the railgun. Voltage measurements were performed with a shunt resistor and a current transformer to avoid any electrical connections to the railgun apparatus.

Exit velocity was measured in a two station break-wire switch which utilized 0.025 mm diameter tungsten wire. The wire switch was shielded by one or more baffle plates to prevent false signals from debris and plasma. Velocity measurements are accurate to better than ±2%. The wire switch velocity is always compared to the velocity determined from magnetic probe data. If there is a significant discrepancy the wire switch data is discarded. This happened in fewer than 10% of the HYVAX tests.

TABLE I: HYVAX DIAGNOSTICS

Quantity Measured	Measurement Technique
Input Current (3)	Rogowski, passive integrator
Input Voltage (3)	Shunt resistor, current transformer
Rail Current (8)	8-slot loop, passive integrator
Muzzle Voltage (1)	Shunt resistor, current transformer
Injection Velocity (2)	He-Ne laser beam, logarithmic detector
Exit Velocity (2)	Tungsten wire screen (1 mil dia.), break mode

Most of the information about plasma armature behavior is obtained from an array of nine magnetic probes installed at 30.5 cm intervals along the barrel. Probe position is shown in Fig. 1. Two probe orientations have been utilized, "arc current sensing" with the loop axis parallel to the rails and "rail current sensing" with the loop perpendicular to the rails. The output from these probes can be recorded directly (signal ∝ $\dot{B}$) or after integration (signals ∝ B). The direct signals provide only qualitative information and were used only on a few early tests. The integrated probe signals give a great deal of insight into the plasma armature behavior. The rail current probe has proven particularly useful for obtaining quantitative information. Because of its importance, the rail current probe is discussed in more detail in the next section.

Rail Current Diagnostic The rail current magnetic probe can provide accurate, quantitative measurements of the current flowing in the rails at a given point. However, these are significant limitations which must be understood when interpeting the measurements. The most important of these limitations are limited spatial resolution, coupling to the plasma current, and time-dependent sensitivity.

Spatial resolution is limited by the distance of the probe from the railgun axis. It can be shown for simple geometries that the probe signal rises from zero to maximum as the plasma moves a distance along the rails approximatley equal to twice the distance of the probe from the rails. Plasma current variations over distances much smaller than twice the rail to probe spacing cannot be observed. For a plasma of finite length, l_p, the apparent length measured by the rise of the magnetic probe signal is given by a sum in quadrature; i.e.

$$l_a = [(2d)^2 + l_p^2]^{1/2} \quad (1)$$

where l_a is the apparent length and d is the probe to axis spacing. Since (1) is derived for simplified rail geometry it is not useful for calculating l_p from values of l_a. However, (1) does show that values of l_a ≥4d are reasonably accurate. For example, a measured value of l_a=4d corresponds to a true plasma length of 3.5d, an error of ≈15%.

For HYVAX the probes are located as shown in Fig. 1 at a distance of 32 mm from the axis. Useful measurements can be made of plasma variations which occur over a distance greater than 10-12 cm.

A rail current probe installed in the position illustrated in Fig. 1 has some coupling to the plasma current. Plasma current coupling produces the negative dip immediately before the current rise which is seen on most of the probe signals in Fig. 2. The amplitude of this signal is sensitive to the sharp gradient in current density at the plasma-projectile interface. When the plasma separates from the projectile this gradient disappears and the negative precursor signal vanishes as shown by signal #9 of Fig. 2. Plasma current complicates the quantitative interpretation of rail current signals and it is best to eliminate it by proper placement of the probe coil (see description of the MIDI-2 diagnostic below).

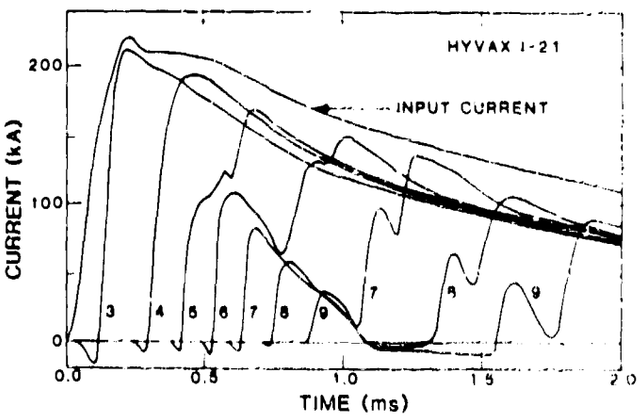

Fig. 2 Magnetic probe signals for HYVAX test I-21

An ideal current sensor provides an output which is exactly proportional to the current flowing in an adjacent rail. In fact, the magnetic probe loop senses local magnetic field, which is a function of the rail current, its distribution over the rail volume, and of induced currents in nearby conductors. For the rail

railgun probe the effect of magnetic field diffusion into the adjacent steel shell results in a time-dependent relationship between output voltage and current. This is illustrated by the calibration data shown in Fig. 3.

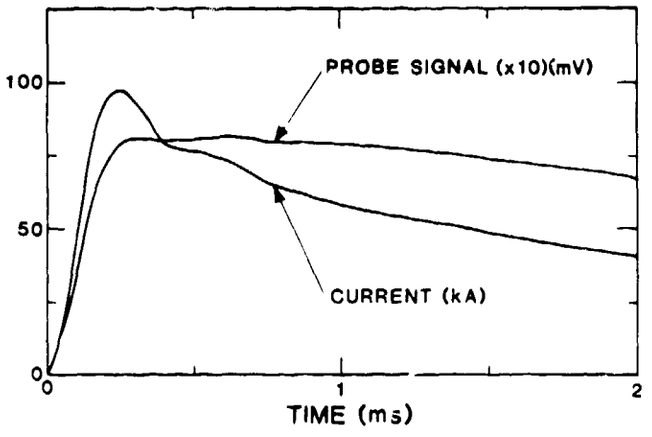

Fig. 3 Time-dependent response of a rail current probe to a known input current

The data of Fig. 3 is taken by shorting the railgun muzzle and discharging the capacitor bank modules at reduced voltage. This simple calibration technique is another advantage of rail current probes. There is no equivalent technique for arc current probes.

Accurately correcting for the time-dependent response is very difficult due to the complex geometry and time dependence of magnetic field diffusion. For simple waveforms an approximate correction can be obtained by assuming a simple exponential time dependence for the field change due to diffusion. This leads to an equation relating current to probe signal of the form

$$V(t)=(A+B)I(t) - B\int_0^t I(\tau)\exp[\alpha(\tau-t)]d\tau \qquad (2)$$

Equation (2) can be used to evaluate the constants A, B, and α by least squares fitting to the calibration data. Once the constants A, B, and α are determined for a given probe the subsequent experimental data can be corrected numerically using the inverse of (2),

$$I(t)=C[V(t)+R\int_0^t V(\tau)\exp[\beta(\tau-t)]d\tau] \qquad (3)$$

where the constants C, R, and β are given by

$$C = (A+B)^{-1} \qquad R = \alpha B/(A+B) \qquad \beta = \alpha A/(A+B)$$

Applied to the calibration data shown in Fig. 3 this correction scheme reduces the factor of 2 discrepancies to less than 5%. For more complex waveforms the correction is not as good, as evidenced by the corrected magnetic probe signals in Fig. 2.

For example, in Fig. 2 there is a clear difference between the probe currents and the input current at late time, although the agreement among probe signals is moderately close. Also the probe #3 and #9 signals fall below the baseline when they should have returned to zero. Nonetheless, this correction does permit semi-qualitative evaluation of the current levels in various arcs which is very difficult using the uncorrected signals.

EXPERIMENTAL RESULTS

Over the past two years 40 experiments have been carried out with the HYVAX railgun. These tests have investigated the influence of various parameters on railgun performance including peak current, insulator material, injection velocity, injection gas, and fusing technique. Overall railgun performance has been reported elsewhere for many of these tests. In this section the results of a single experiment will be examined in detail.

The test conditions for HYVAX test I-21 are summarized in Table II. The magnetic probe data for this test are shown in Fig. 2. To aid in the interpretation of the experiment the magnetic probe data, the wire switch times and muzzle voltage signal are presented on a position-time (x-t) diagram in Fig. 4.

TABLE 2: EXPERIMENTAL CONDITIONS FOR HYVAX I-21

Projectile:	Lexan 11.1 mm dia. x 11 mm long mass = 1.3 grams.
Injector:	Chemical propellant v_i = 1.13 km/s
Fuse:	Iron, mass = 0.1 g
Railgun:	L' = 0.3 μH/m Effective length = 2.1 m Current = 210 kA (Fig. 2) Initial air pressure = 50 Torr
Exit velocity:	3.08 km/s

The horizontal lines labeled B3-B9 in Fig. 4 are drawn at the position of the corresponding magnetic probe. On each of these lines the times of rapidly increasing probe signal (high current density) are shown by a thickening of the line. The line labeled M marks the position of the muzzle. The accented region on this line indicates the muzzle voltage spike produced when a current carrying plasma exits the muzzle. The points WS1 and WS2 show the time and position when wire switch #1 and #2 were broken. The initial position and velocity of the projectile, as determined from the laser detection system, are shown by a short line segment extending to the left of the t=0 axis.

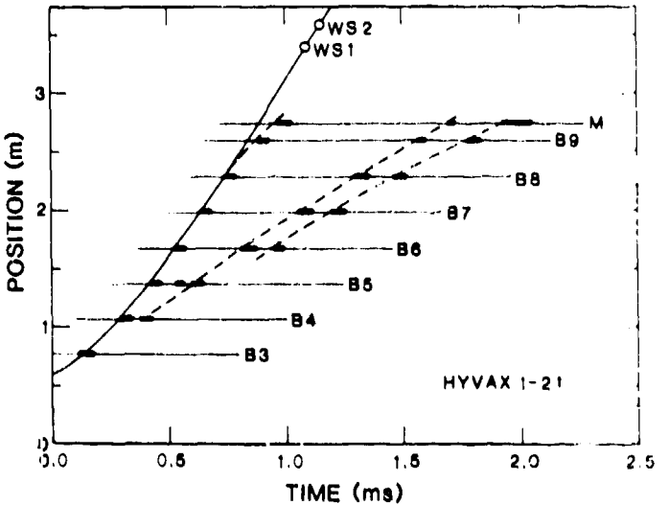

Fig. 4 Position-Time plot for HYVAX test I-21 (—projectile, --arc front)

To aid in visualizing the motions occurring in the railgun the projectile path is marked by a solid line and the leading edge of each high current arc region is connected by a dashed line.

Arc length The length of each high current arc

can be determined from Fig. 4 by drawing a second line the rear edge of each of the accented regions. The vertical distance between this line and the line connecting the front edges gives the arc length. This procedure gives an arc length of 8 to 10 cm for all of the arcs in Fig. 4. Since the probe resolution is only 10-12 cm all that can be inferred is that the region of high current density is less than 10 cm long.

Examining the lower current density regions gives a somewhat different picture. Comparing the signals from probes #3 and #4 in Fig. 2 it is apparent from the slower rise and rounded top that the arc passing probe #4 has a long tail of low current density. The end of this tail passes probe #4 at 450 μs when the primary arc has already passed probe #5, approximately 30 cm away.

The short, high current density arc is leaving behind it a region filled with partially ionized, weakly conducting gas. This region is bounded on the back edge by the high pressure, neutral gas from the injector.

This picture of a high current arc followed by a weakly conducting residue seems to be characteristic of plastic insulators, particularly pure Lexan. Tests with Mycalex, a mica-glass material, produce almost uniform current density throughout the region the arc traverses. The reason for this difference is not understood. It may be a function of the atomic composition of the plasma, particularly the large amount of hydrogen from the plastics. Another possibility is that the plasma is being cooled by neutral gas vaporized from the plastics by a combination of stored heat and heat transfer from the partially ionized gas.

Restrike A long tail of weakly conducting plasma does not by itself degrade railgun performance. Unfortunately this situation is not stable. It is apparent from the signal on probe #5 that a region of high current density has develop near the back edge of the conducting region.

The instability which causes the trailing or "restrike" arc involves the I-V characteristic of gas discharges and the motion of the gas behind the arc. In general, gas discharges exhibit a minimum operating voltage at a particular current density, with higher voltages required for both increased and decreased current density. The voltage increase is usually small as current is decreased (small negative resistance). Therefore, small voltage changes can result in large changes in the current density.

The voltage increase which creates the restrike arc is generated by the velocity difference between the main arc and the trailing plasma. The weakly ionized gas behind the arc is moving more slowly as is clearly shown by the velocity of the restrike arc in Fig. 4. The mechanism responsible for slowing this gas may be simple viscous drag or may be mixing drag due to neutral vapor emitted by the walls after the primary arc passes.

Regardless of the slowing mechanism there is a substantial velocity difference between the primary arc front and the low current tail region. At 300 μs, when the main arc passes probe #4 it is carrying a current of approximately 180 kA at a velocity of 2 km/s. At the same time the rear surface of the ionized region is moving at about 1.2 km/sec. This velocity difference generates a voltage $V_p = L'Iv = 43$ volts. This voltage is sufficient to initiate a restrike arc in the MYVAX railgun (fiberglass-copper).

By 450 μs the main arc current has fallen to 110 kA. The velocity difference is 2.4-1.5=0.9 km/s and the inductive voltage is 30 volts. Since both the main arc and the restrike arc are now operating at high current density (and nearly equal voltages) this inductive voltage acts to reduce the current in the main arc.

Consider a closed circuit through the restrike arc, along one rail, through the main arc and back along the second rail. The sum of all the voltages must equal zero. Since the arc voltages are nearly equal and the resistive drop in the rails is small the two inductive components must cancel. That is:

$$V = \frac{d}{dt}(LI) = L'I(\Delta v) + L\dot{I} = 0 \qquad (4)$$

Solving (4) for $\dot{I}$ gives:

$$\dot{I} = \frac{-L'\Delta v}{L} I = -\frac{(\Delta v)}{\ell} I \qquad (5)$$

where ℓ is the separation between the two arcs. The calculated value of $\dot{I}$ from (5) is $\dot{I}_{calc} = -2.9 \times 10^8$ A/s.

The experimental value deduced from Fig. 2 is -2.5×10^8 A/s, somewhat lower than the simple calculation predicts. Nonetheless, the conclusion is inescapable. Once a restrike arc has formed the velocity difference between it and the main arc will cause a continuous decrease in the main arc current.

The importance of the velocity difference was revealed dramatically in recent experiments which investigated a static fuse built into the wall of the railgun. When this fuse is vaporized a large fraction of the fuse material is only weakly ionized and is left at rest while the primary arc accelerates to the projectile velocity (~1 km/s). In this case a restrike arc has already formed before the main arc passes probe #3.

Restrike arc velocity Since the velocity difference between the main arc and the restrike arc initiates restrike, it is important to understand why the restrike arc moves so slowly. The argument has been made many times that the restrike arc should accelerate and catch up with the main arc. It does not and the reason appears to be vaporization (not ablation) of wall material after the primary arc passes.

For simplicity, consider the situation shown in Fig. 4 at 1.2 ms, when both the projectile and the main arc have left the barrel. The first restrike arc is carrying a current of 90 kA and the magnetic force exerted on it is 1215 N. Since the restrike arc is not accelerating this force must be balanced by some drag force.

The ablation drag can be estimated using the ablation model of [2]. For the measured arc voltage, current and velocity $F_{ab} = \dot{m}v = 290$ N. This accounts for 24% of the required drag force. Since the restrike arc is quite short and moving slowly the viscous drag on it is negligible. A plausible explanation for the missing drag force is residual gas in the railgun bore which is being pushed along by the restrike arc.

If a residual gas of density δ, moving at velocity v_g is swept up by an arc moving at velocity v_p a drag force

$$F = \dot{m}\Delta v = \delta \pi r^2 (v_p - v_g) v_p \qquad (6)$$

is exerted on the arc.

Assuming $v_g = 0$, the gas density required to account for the observed velocity is 4 mg/cm^3. To evaporate this much plastic from the wall requires an energy of approximately 20 Joules/cm of length.

When the primary arc passed this point in the barrel, the energy dissipated in the arc was on the order of 2 MJ, sufficient to ablate and ionize about 1 mg/cm^3 of wall material. Over half of this energy goes into ionization. If a significant fraction of this material subsequently cools by conduction and radiation (ions and electrons recombine, most of the ionization energy will be converted to heat. It appears plausible therefore that the 20 J/cm required to vaporize 4 mg/cm^3 of plastic into the bore is available. However experimental and theoretical work is needed to test this hypothesis, particularly a measurement of the arc

of neutral gas ejected following the primary arc. Also a more detailed calculation of the viscous drag forces involved in pushing this residual gas through the barrel is needed.

The velocity of the restrike arc depends upon two other experimental factors, injector gas and venting. Changing injection gas from gun powder products to helium causes a small increase in restrike arc velocity, probably because a higher sound speed allows the helium to push against the rear surface of the arc more effectively. This is a small effect and has no observed consequences for railgun performance.

Venting of the railgun bore has a significant effect on restrike arc velocity. Several experiments were carried out with HYVAX using two barrel sections which had longitudinal cracks in the insulator for nearly the full length. These cracks were the result of an earlier test and their width was uncontrolled. Experimentally, it was observed that a significant amount of carbon was blown into these cracks and once a magnetic probe was blown out of the gun by gas venting through these cracks.

The effect of the cracks on restrike arc velocity is shown in Fig. 5. During projectile acceleration the restrike arc is moving 1.8-2.0 km/s compared to 1.2-1.4 for the non-vented test. After the projectile exits the gun the restrike arc accelerates to 3 km/sec in contrast to the continual slowing observed without venting. The higher restrike arc velocity reduces the inductive voltage difference between the two arcs. This results in less transfer of current to the restrike arc. At exit time the main arc current for the vented test is 80 kA, and the arc has not separated from the projectile. Without venting the main arc current has decreased to 48 kA and the arc has separated from the projectile.

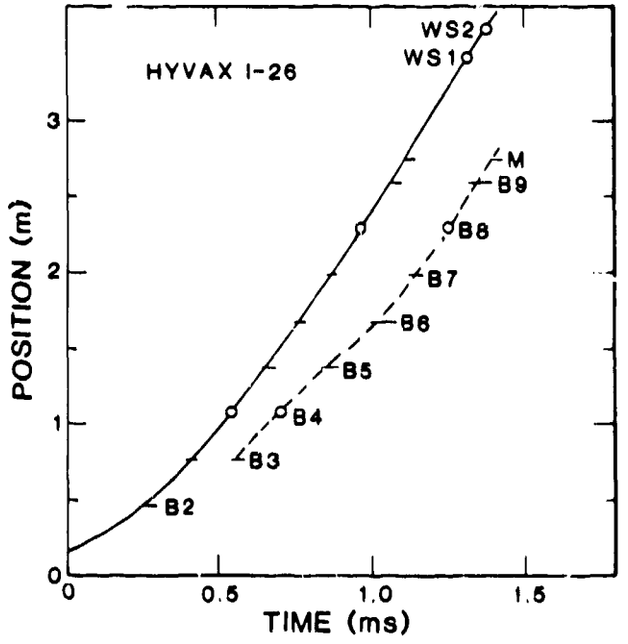

Fig. 5 Position-Time plot for test I-26 (Vented)

Unfortunately these striking velocity differences do not have a significant overall effect on performance. The energy delivered to the projectile in the vented test was increased about 9% over the non-vented tests. Also, it seemed venting did not have any measureable effect on the primary arc, probably because the crack opened under the combined influence of gas pressure and magnetic forces after the primary arc passed.

MIDI-2 EXPERIMENTS

MIDI-2 Railgun

The Los Alamos MIDI-2 railgun is the second experimental device built primarily to investigate material effects. The design emphasizes easy replacement of internal parts and high quality diagnostics rather than high performance.

A cross-section of MIDI-2 is shown in Fig. 6. The outer containment shell is a 15 cm o.d. x 7.5 cm i.d. fiberglass cylinder 1.83 meters long. It is split the full length, and stainless steel bolts are used to close this gap and compress the internal structure. The rail and insulator elements are supported by four identical quadrant pieces made of G-10 fiberglass. By eliminating all metal components except the compression bolts, the time dependent perturbation of the magnetic probe signals results solely from current diffusion into the rails, a 20% effect. The bore is nominally square, 9.5 mm x 9.5 mm. The 9.5 mm thick x 19 mm wide copper rails provide a calculated, L' of 0.32 μH/m. The structure is vacuum tight to a pressure of 650 m Torr.

Electrical power is provided by one module of the HYVAX capacitor bank. Maximum design current is 150 kA. After allowing for a connection region in the breech the useable length is 1.64 m. At the present time there is no injection capability.

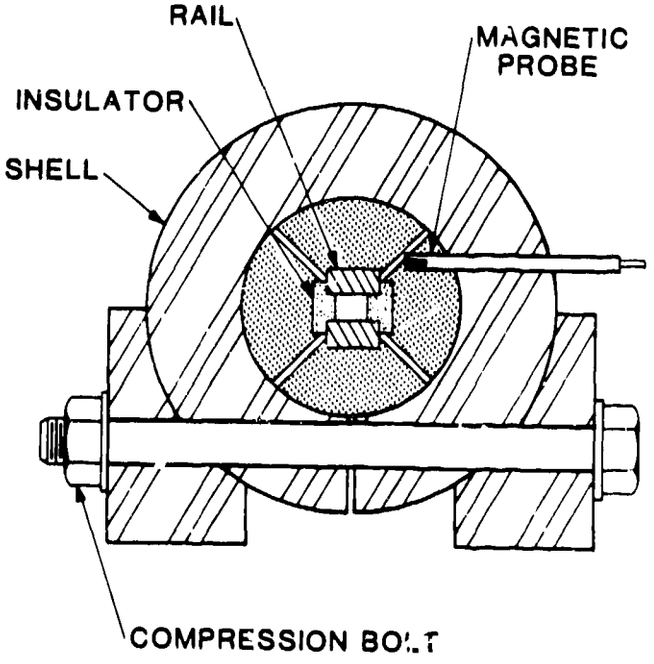

Fig. 6 Cross-section of the MIDI-2 railgun

Diagnostics The diagnostics utilized with MIDI-2 are substantially the same as those used on HYVAX. The design and placement of the magnetic probes has been changed to eliminate coupling of the arc current magnetic field into the rail current sensor.

The HYVAX magnetic probes are located on the midplane between the two rails with the normal vector of the coil oriented in the y direction (see Fig. 2). To eliminate coupling to the arc current the sensing coils in MIDI-2 are oriented in the x direction, parallel to the arc current. Since there is no x component of the rail magnetic field on the midplane it is necessary to move the coils off of the midplane as shown in Fig. 6. The optimum distance off the midplane was determined by calculating the x component of the magnetic field

for uniform current in the rails.

This improvement, plus the non-conducting shell, has greatly increased the accuracy of rail current measurements. Fig. 7 presents typical data from a MIDI-2 test. The signals have been corrected using the technique described previously. Both the agreement among magnetic probe signals, and the agreement between magnetic probe current and input current at late times, is better than ±3%. Also, the new probe position has eliminated the negative precusor signal, as expected.

A total of ten magnetic probes are installed on MIDI-2. To improve resolution during the initial arc motion the spacing is non-uniform. The probe positions, relative to the initial fuse location are 5, 12, 22, 35, 50, 65, 85, 110, 135 and 160 cm.

Experimental Results Only six test have been performed with the MIDI-2, all directed at better understanding the effect of insulator material on railgun performance. Because the high velocity interaction between arc plasma and insulator is the area of greatest uncertainty at this time, most of these tests were performed in the "free-arc" mode. These tests are performed without any projectile. A fine copper wire fuse (mass = 2mg) is vaporized to form the plasma, which is then accelerated very quickly to high velocity. This type of test cannot be performed with the railgun completely evacuated because a small fraction of the arc material will be accelerated to very high velocity and initiate a stationary arc when it reaches the muzzle. To prevent this the railgun is backfilled to a low pressure. The air creates a well defined arc front.

The experiment is called "free arc" in the sense that the forces on the arc from the low pressure air are substantially less than the forces to be measured, i.e. ablation and viscous drag. A simple criterion for "free arc" behavior can be established by calculating the velocity achievable if only the forces due to the air were present. The air generates two forces, $\dot{m}v$ and viscous drag. Equating these forces to the magnetic force gives

$$\frac{1}{2} L'I^2 = \left[\rho h^2 + \frac{2C_f M_a}{h}\right] v_m^2$$

where ρ = initial air density
h = bore height
C_f = friction coefficient (= 0.003)
M_a = mass of accumulated air.

For the MIDI-2 experimental condition (initial air pressure = 10 Torr, I = 100 kA), the calculated maximum velocity is 23 km/s. As long as the experimental velocity is substantially below 23 km/s the arc can be considered "free" from forces arising from the initial air fill. Experimental verification of the "free arc" condition can also be obtained by varying the initial air pressure.

The four "free arc" tests were performed using insulators made of G-10, Lexan, polyvinyl chloride (PVC) and polyethylene. A typical set of magnetic probe traces is shown in Fig. 7 for the PVC insulator. Analysis of all four tests gave similar results. The arc is accelerated from rest to a velocity of 8-11 km/s during the rising portion of the current pulse (0-150 μs, 0-80 cm) and then travels at constant velocity for the remainder of the barrel length.

The final velocity achieved is different for each material; G-10, 8.2 km/s; Lexan, 8.9 km/s; PVC, 7.9 km/s and polyethylene; 11.1 km/s. The higher velocities correlate with decreasing molecular weight as expected for ablation dominated motion. A preliminary comparison with ablation model predictions has been made using the LARGE railgun code and is reported in a companion paper [4].

In the following discussion the experimental observations from the MIDI-2 tests will be compared to the HYVAX results described earlier.

There are substantial differences between the plasma conditions in MIDI-2 and in HYVAX. The most important difference is the lower plasma density resulting from the absence of a projectile and from a lower current. This causes the plasma voltage to be lower, 100-120 v compared to 180-200 volts in HYVAX. The second difference is the high velocity. The residence time of the arc in a given location is so brief that no observable damage is done to the copper rails for the first 130 cm of arc motion. This agrees with the LARGE code prediction that copper ablation does not occur at high velocity. Despite these differences the magnetic probe results from MIDI-2 are very useful because the close probe spacing and increased accuracy give a more detailed look at plasma development.

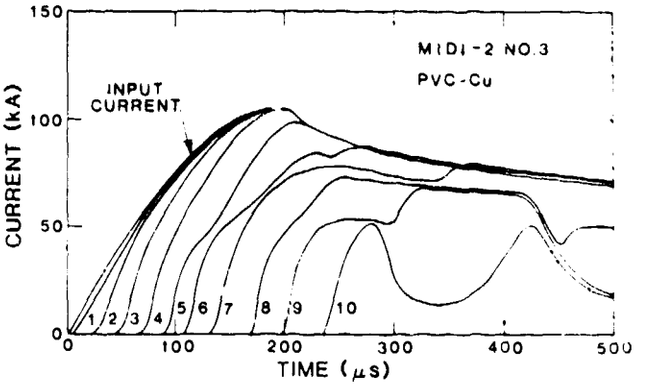

Fig. 7 Rail current probe data from MIDI-2 test #3

Arc length The spatial development of the plasma can be obtained from the data of Fig. 7. The vertical height between two probe curves at a given time is a measure of the plasma current flowing in the region between those two probes. Table III presents these current differences at nine different times. For convenience the times chosen correspond to the time the plasma front arrives at each probe location.

For example, at 50 μs the plasma is just reaching probe #3. At that time 30 kA is flowing in the plasma region between probes 2 and 3 (10 cm) and 10 kA in the region between probes 1 and 2 (7 cm). The plasma is approximately 15 cm long at 50 μs.

At 110 μs, when the plasma has reached probe #5, there is a significant current flowing in the region from probe #3 to probe #5, a length of 43 cm. At 110 μs the current density has apparently reached the minimum value which gives a positive dynamic resistance characteristic. The inflection in probe signal #5 at 40 kA marks the beginning of a separation into two distinct current carrying regions. The entries in Table III for times greater than 110 μs show a clear pattern of two current carrying regions.

Fig. 7 also shows a second separation later in time. The inflection is first seen on probe #8 at about 300 microseconds. The signal on probe #9 shows two distinct plasma regions at 210 and 310 microseconds. The development and motion of these restrike plasma regions can be seen more clearly in Fig. 8.

The range of stable plasma current density can be estimated from the magnetic probe data. The initial current risetime for each probe, combined with the measured velocity, yields an arc length of approximately 14 cm. This implies a maximum current density of 3 kA/cm². The minimum stable current density can be calculated from the current flowing in the region between probes #4 and #5 at 110 μs (just before formation of the restrike arc). The minimum current density is 22 kA/15 cm = 1.5 kA/cm². Current densities for

1.5 to 3 kA/cm^2 correspond to the minimum operating voltage at MIDI-2 conditions of temperature, density and composition. In HYVAX experiment I-21 the stable current density is greater than 10 kA/cm^2.

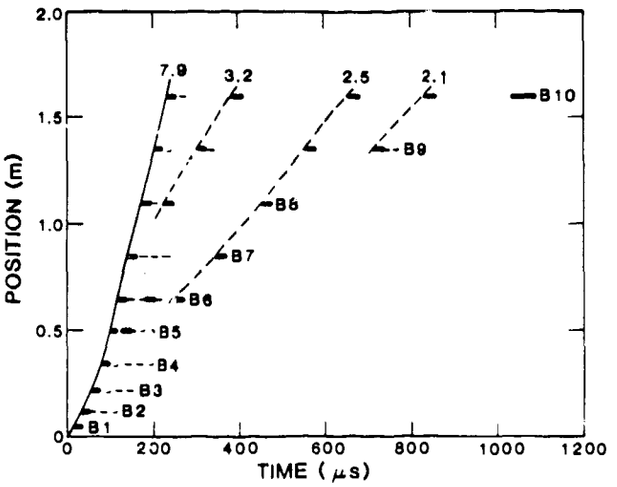

Fig. 8 Position-Time plot for a "free arc" test on MIDI-2

The relationship between current density and electric field and its dependence on local conditions must play an important role in any improved model of the plasma armature. At present the information required to quantify this relationship is not available and further experimental work is needed.

TABLE III: CURRENT DISTRIBUTION AT VARIOUS TIMES FOR MIDI-2, TEST #3

Time	1-2	2-3	3-4	4-5	5-6	6-7	7-8	8-9	9-10
29 μs	20 kA								
50	10	30							
72	3	15	38						
92	3	8	23	36					
110	2	4	17	22	34				
136	1	3	9	27	6	46			
172			3	17	20	6	56		
200				8	20	5	23	48	
240					9	4	8	19	52

Restrike Voltage The inductive voltage developed by the primary arc is substantially higher for the MIDI-2 experiments than for HYVAC-2 experiments. For example, at 100 microseconds, the inductive voltage developed is (75 kA) $(0.324 \times 10^{-6})(7.6 \times 10^{3})$=186 volts relative to a stationary conduction path near the fuse position in the breech. In HYVAX experiments, restrike occurred near the fuse position at a voltage of less than 40 volts. This contrasts markedly with the absence of restrike at a voltage of 80 v in the MIDI tests.

The difference in breakdown voltage may be due to the low plasma density in the MIDI-2 experiments, however, there are two additional experimental observations which suggest an alternative explanation. In one experiment on MIDI-2, a loose joint in the breech caused some minor arcing in the breech region. In a second experiment a low mass projectile was employed which slowed the arc. In both cases the copper rail surface was melted locally by the discharge. In both cases restrike arcs were observed at a lower voltage in the region of melting. These observations suggest that the voltage required to initiate conduction is substantially higher in the absence of surface melting on the copper rails. Further investigations of this effect, with particular attention to alternative rail materials, may help in reducing restrike for some applications. However, it is unlikely that improved electrode conditions will increase the breakdown voltage more than 150 to 200 volts since most metals will support a high current density glow discharge at voltages of 150 to 200 volts.

Restrike Arc Velocity. The restrike arc velocity is higher in the MIDI-2 experiments than in the HYVAX experiments. According to Fig. 8 the velocity of the first restrike arc is 3.2 km/s, and the second arc reaches 2.5 km/s. This compares to only 1.2 to 1.4 km/s in the HYVAX experiments. The low restrike arc velocity in HYVAX experiments was attributed to neutral residue left in the bore by the primary arc. This explanation is supported by the MIDI-2 results.

In Table IV, the velocity of several restrike arcs is tabulated along with the energy dissipated by the preceeding arc. There is a clear correlation between the energy available to generate residual gas and the velocity of the following restrike arc. Attempts to quantify this relationship have met with limited success. The complexity of the physical processes involved in energy transfer and turbulent flow in the residual gas make comparison among different railguns and different experimental situations very difficult.

TABLE IV: COMPARISON OF RESTRIKE ARC VELOCITY WITH ENERGY DISSIPATED IN PREVIOUS ARC PASSAGE

Experiment	Restrike Velocity	Dissipated Energy
HYVAX	1.2 km/s	56 J/cm
MIDI-2	3.2 km/s	8 J/cm
	2.5 km/s	20 J/cm
	2.1 km/s	26 J/cm

CONCLUSIONS

A detailed examination of measured current waveforms from HYVAX and MIDI-2 tests provides strong evidence that simple ablation [2,3] is only a first order model. The weakest element of the simple ablation model is its assumption of a uniform current density in the plasma. Experiments show that uniform current density is a valid assumption only at early times before viscous drag and vaporization have created a strong velocity gradient along the length of the arc. Once a substantial velocity gradient is established, a restrike arc develops, diverting current from the primary arc and reducing railgun performance. In many cases the restrike arc causes a greater performance loss than direct ablation processes.

Restrike is not a separate mechanism distinct from ablation, but is an indirect consequence of the ablation process. Ablation generates the residual material behind the primary arc which retards the motion of the restrike arc. The velocity difference between primary and restrike arc causes a voltage difference which decreases the current in the primary arc. From another point of view, the restrike arc is only a liability if it has material, other than the projectile, to plow against. Ablation provides that material.

The HYVAX and MIDI-2 experiments provide evidence to support the following improved model of the ablation process.

1) The high temperature plasma ablates a small amount of mass from the wall. This material is fully ionized and causes an ablative drag.

2) Viscous drag acts on the arc boundary, slowing and cooling some fraction of the ionized gas.

3) The heat transferred to the wall as this gas

rial cools causes further vaporization of the wall material. Due to the lower temperature this material is only weakly ionized.

4) Mixing of the vaporized material into the tail of the main arc increases the drag and further lowers the temperature.

5) Ionic and molecular recombination releases stored energy which is available to vaporize more wall material.

6) The final state of the gas in the bore behind the primary arc (temperature, density, fractional ionization, and velocity) is a complex function of the wall material, the primary arc power and velocity, and the electromagnetic environment.

7) The electric field acting on the partially ionized gas at each point in the bore is a function of the relative velocity of the plasma and the magnetic field.

8) Current density, power input, and ionization rate at each point depend on local electric field, atomic composition, electron density, neutral density and temperature. When a critical electric field (or power input) is exceeded, current increases rapidly forming a localized restrike arc.

Unfortunately this improved model is virtually useless for providing intuitive guidance in the design and improvement of future plasma armature EMLs. For example, the simple ablation model predicts that a low molecular weight material, such as polyethylene, will give the lowest armature drag. However, plastics have a low vaporization energy, thus generating larger amounts of residual gas in the bore and increasing the drag on any restrike arc. The relative importance of these two effects varies with the details of the wall materials, the projectile velocity and the driving current. Choosing the best insulator material requires either detailed calculation or trial and error evaluation.

The number of factors influencing plasma behavior and the complexity of their interaction precludes application of the improved model in railgun codes like LARGE which attempt to provide an overall calculation of launcher performance. It appears that further progress in understanding plasma armature EMLs will require the development of a specialized calculational model which can address time-dependent electrical, thermal, chemical and mechanical processes in at least one spatial dimension. The alternative is to move toward EML designs which decouple the electrical system from the restrike region (some form of segmentation) or to develop a non-plasma armature.

REFERENCES

(1) S. C. Rashleigh and R. A. Marshall, J. Appl. Phys. 49 (1978) 2540

(2) J. V. Parker, W. M. Parsons, C. E. Cummings and W. E. Fox, "Performance Loss Due to Wall Ablation in Plamsa Armature Railguns", presented at the AIAA 18th Fluid Dynamics and Plasma Dynamics and Lasers Conference, July, 1985, Cincinnati, OH. Paper AIAA-85-1575.

(3) N. M. Schnurr and J. F. Kerrisk, "Numerical Studies of Ablation and Ionization of Railgun Materials", Op. Cit. Paper AIAA-8541575.

(4) N. M. Schnurr and J. F. Kerrisk, "Numerical Predictions of Railgun Performance Including the Effects of Ablation and Arc Drag", presented at the 3rd Symposium on Electromagnetic Launch Technology, April, 1986, Austin, TX.